



Published in final edited form as:

J Biol Chem. 2007 March 2; 282(9): 6183–6191. doi:10.1074/jbc.M608863200.

Oxidoreductase Interactions Include a Role for ERp72 Engagement with Mutant Thyroglobulin from the *rdw/rdw* Rat Dwarf*

Shekar Menon[‡], Jaemin Lee[§], William A. Abplanalp[‡], Sung-Eun Yoo[‡], Takashi Agui[¶], Sen-ichi Furudate^{||}, Paul S. Kim[‡], and Peter Arvan^{§1}

[‡]Program in Cell and Molecular Biology and Division of Endocrinology, University of Cincinnati, Ohio 45267

[¶]Laboratory of Experimental Animal Science, Graduate School of Veterinary Medicine, Hokkaido University, Sapporo, Hokkaido 060-0818, Japan

^{||}Department of Laboratory Animal Science, Kitasato University School of Medicine, Sagami-hara, Kanagawa 228-8555, Japan

[§]Division of Metabolism, Endocrinology & Diabetes, University of Michigan Medical Center, Ann Arbor, Michigan 48109

Abstract

Newly synthesized thyroglobulin (Tg), the secretory glycoprotein that serves as precursor in thyroid hormone synthesis, normally forms transient covalent protein complexes with oxidoreductases of the endoplasmic reticulum (ER). The Tg-G2320R mutation is responsible for congenital hypothyroidism in *rdw/rdw* rats, in which a lack of secondary thyroid enlargement (goiter) implicates death of thyrocytes as part of disease pathogenesis. We found that mutant Tg-G2320R was retained within the ER with no detectable synthesis of thyroxine, had persistent exposure of free cysteine thiols, and was associated with activated ER stress response but incomplete ER-associated degradation (ERAD). Tg-G2320R associated with multiple ER resident proteins, most notably ERp72, including covalent Tg-ERp72 interactions. In PC C13 thyrocytes, inducible overexpression of ERp72 increased the ability of cells to maintain Tg cysteines in a reduced state. Noncovalent interactions of several ER chaperones with newly synthesized Tg-G2320R diminished over time in parallel with ERAD of the mutant protein, yet a small ERAD-resistant Tg fraction remained engaged in covalent association with ERp72 even 2 days post-synthesis. Such covalent protein aggregates may set the stage for apoptotic thyrocyte cell death, preventing thyroid goiter formation in *rdw/rdw* rats.

The endoplasmic reticulum (ER)² serves as the compartment that initiates secretory protein biosynthesis and provides both a more oxidizing environment than the cytosol for promotion

*This work was supported by National Institutes of Health Grants DK40344 (to P. A.) and DK52076 (to P. S. K.) and a Veterans Affairs Merit Award (to P. S. K.).

1 To whom correspondence should be addressed: Div. of Metabolism, Endocrinology & Diabetes, University of Michigan Medical School, 5560 MSRB2, 1150 W. Medical Center Dr., Ann Arbor, MI 48109-0678. Tel.: 734-936-5505; Fax: 718-936-6684; E-mail: parvan@umich.edu.

²The abbreviations used are: ER, endoplasmic reticulum; ERAD, ER-associated degradation; Tg, thyroglobulin; PERK, protein kinase-like ER-resident kinase; IP, immunoprecipitation; PDI, protein disulfide-isomerase; T₄, L-thyroxine; TUNEL, deoxynucleotidyl transferase-mediated dUTP nick end labeling; PEG, polyethylene glycol; DMEM, Dulbecco's modified Eagle's medium; PBS, phosphate-buffered saline.

of disulfide bond formation as well as ER molecular chaperones that facilitate folding of secretory pathway polypeptides (1). Secretory polypeptides that fold to a native conformation become eligible for anterograde transport, whereas those that fail to fold correctly are retained within the ER until they either achieve an acceptable conformation or are targeted for ER-associated degradation (ERAD) (2). These processes of ER quality control (3) help to prevent secretory protein congestion of the ER lumen that can adversely affect secretory pathway efficiency.

A growing list of genetic diseases have been accounted for by structural changes in secretory proteins that alter their folding and render them deficient for ER export (4). Many of these ER storage diseases produce a simple deficiency of the secreted protein (5), whereas others may be cytotoxic to cells that attempt to produce them (6).

Preventing toxic accumulation of misfolded secretory proteins, for example via ERAD, is vital for proper ER homeostasis and may be a strategy for therapies of ER storage diseases (7,8). ERAD is built around highly conserved mechanisms that target misfolded proteins for intracellular disposal (9). Key steps in this pathway include recognition of the ERAD substrate for unfolding and targeting for retrotranslocation to the cytosol (10) followed by proteolysis via the ubiquitin-proteasome system (11). An inability to effectively degrade mutant secretory (or membrane) proteins may result in a gain-of-toxic-function that leads to cell death. This can occur either in an autosomal dominant manner, such as occurs with familial neurohypophyseal diabetes insipidus (12) or in an autosomal recessive manner, such as in patients expressing the Z-variant of $\alpha 1$ -antitrypsin (13).

Thyroglobulin (Tg), the major secretory glycoprotein of thyrocytes that serves as the precursor protein for thyroid hormone synthesis, begins to fold in the ER (14,15) with the assistance of multiple molecular chaperones (16,17) including endogenous oxidoreductases that transiently form covalent, mixed disulfides with nascent Tg (18). Tg deficiency is a well recognized cause of congenital hypothyroidism (19) in which disease-causing Tg mutants are blocked in ER export and then are routed for proteasomal degradation (20). Consequently, the thyroid gland develops hypertrophy and hyperplasia (goiter) secondary to chronic elevation of thyroid stimulating hormone (21). However, recent genetic linkage analyses have found the thyroglobulin gene region as a major locus in human familial congenital hypothyroidism even in the absence of goiter formation (22). Moreover, in the *rdw/rdw* rat dwarf (23), homozygous expression of the Tg-G2320R mutant (24,25) does not lead to goiter but rather to a hypoplastic thyroid gland (26), suggesting a possible gain-of-toxic-function in affected thyrocytes.

In this study, we have investigated the Tg-G2320R mutant protein and found persistent cysteine thiol exposure consistent with thiol-mediated ER retention (27), activation of the ER stress response, and extensive but incomplete ERAD with a small degradation-resistant fraction remaining engaged in covalent complexes with ERp72 for days, if not longer. Evidence is provided to suggest that ERp72 might function as a thiol reductase in the ER, and because interaction with ERp72 has recently been shown to inhibit ERAD of mutant Tg (28), these interactions might potentially predispose to toxicity of thyrocytes in *rdw/rdw* rats.

EXPERIMENTAL PROCEDURES

PEG-Maleimide Treatment

Incubation was performed in Cys/Met-free DMEM containing 10 mM mPEG 5000-maleimide (SunBio) for 75 min at 37 °C. The samples were then boiled for 1 min in a buffer containing 1% SDS, 2% 2-mercaptoethanol, 0.1 M NaCl, 25 mM Tris, pH 6.8.

Silver Staining and Detection of ER Chaperones and T₄

Thyroid homogenates were freshly prepared by boiling for 5 min in a buffer containing 4% SDS, 2% mercaptoethanol, 10 mM Tris, pH 6.8. After SDS-PAGE, samples were electrotransferred to nitrocellulose before immunoblotting with respective chaperone antibodies or anti-T₄ antibody (Sigma) followed by horseradish peroxidase-conjugated secondary antibodies. Bands were visualized with enhanced chemiluminescence.

Immunofluorescence of Phospho-PERK

Paraffin-embedded wild-type and *rdw/rdw* rat thyroid paraffin sections (10 μm) were placed on coated glass slides and deparaffinized by three successive immersions in xylene for 10 min. The sections were rehydrated for 5 min each in a decreasing alcohol series (100, 90, 70% ethanol) and finally immersed in PBS for 5 min. The sections were then incubated in PBS-based blocking solution (5% goat serum) for 5 min at room temperature. Rabbit anti rat-phospho-PERK (Thr-980) from Cell Signaling Technology (catalog no. 3191) was incubated overnight in a humidity chamber at room temperature. The slides were then washed three times in PBS before incubating them with goat anti-rabbit Alexa 488 (Molecular Probes) for 1 h. The slides were then washed three more times in PBS, rinsed with water, and mounted with ProLong anti-fading medium on top of the sample.

Site-directed Mutagenesis of Mouse Tg cDNA

Full-length mouse Tg cDNA was cloned into pcDNA3.1A. Mutations were introduced using the QuikChange™ site-directed mutagenesis kit (Stratagene, La Jolla, CA), and the presence of the mutations was confirmed by DNA sequencing.

Transient Transfection and Stable Cell Lines

COS-7 cells were grown in complete DMEM containing 10% fetal bovine serum and 100 units/ml penicillin/streptomycin (Invitrogen). Cells were transfected with 0.8 μg of plasmid DNA per well using Lipofectamine 2000 (Invitrogen) as per the manufacturer's protocol. Pulse-chase experiments were performed 36 h after transfection.

PC Cl3 rat thyroid cell lines were grown in complete Coons F12 medium supplemented with 5% fetal bovine serum and 100 units/ml penicillin/streptomycin plus a four-hormone mixture (10 milliunits/ml thyrotropin, 10 μg/ml insulin, 5 μg/ml apotransferrin, 10 nM hydrocortisone).

G418-resistant PC Cl3 thyrocytes engineered for constitutive expression of the reverse tet transactivator, called rtTA-7 cells (35), were kindly provided by Dr. James Fagin (Memorial-Sloan Kettering Cancer Center, New York). These cells were maintained in PC Cl3 complete growth medium plus 100 μg of G418. The mouse ERp72 cDNA (from Dr. M. Green, Saint Louis University, MO) subcloned to the BamHI site of pTRE2 (Clontech, Palo Alto, CA) was transfected into rtTA-7, and stable expressors were selected for both hygromycin resistance and doxycycline-inducible expression of ERp72 protein by immunoblotting. rtTA-7-ERp72 cells were maintained in PC Cl3 complete growth medium plus 150 μg/ml and 100 μg/ml G418.

Metabolic Labeling and Immunoprecipitation

Transfected COS-7 cells were starved for 30 min in Met/Cys-free DMEM and then labeled for 1 h at 37°C with 80 mCi/ml of [³⁵S] Easytag™ express protein labeling mix (PerkinElmer Life Sciences). Following pulse labeling, the cells were washed twice with PBS containing Ca²⁺ and Mg²⁺ and chased with DMEM supplemented with an excess of cold methionine and cysteine. When indicated, 15 μM MG132, 100 μM kifunensine, 1 mM 1-deoxymannojirimycin, 1 mM castanospermine, or 10 μg/ml brefeldin A was included in pretreatment, pulse labeling,

or chase incubations. At the end of each chase period, the medium was aspirated, and the labeled cells were treated with ice-cold PBS containing 50 mM iodoacetamide (Sigma) for 10 min to alkylate free cyteine thiols *in situ*. Labeled cells were then lysed for 1 h on ice in 1 ml of IP buffer (1% Triton X-100, 25 mM Tris-HCl, 0.1 M NaCl, pH 6.8) containing a protease inhibitor mixture (29), and 5 units/ml apyrase (Sigma). Nuclei and cell debris were pelleted at 4000 rpm for 10 min at 4 °C. The supernates were then preincubated with zysorbin-protein A (Zymed Laboratories, San Francisco, CA) for 1 h before immunoprecipitation or co-precipitation overnight with the respective antibodies and zysorbin at 4 °C. The immunoprecipitates were washed three times with immunoprecipitation (IP) buffer, boiled in SDS-gel sample buffer, and the supernates were subjected to SDS-4% PAGE. The gels were dried, and Tg bands were visualized by phosphorimaging with quantitation done using ImageQuant 5.0 software (GE Healthcare).

Polyclonal rabbit antisera against BiP, calnexin, ERp72, PDI, and ERp57 were directed against 18–22 amino acid sequences at the C termini of the respective proteins. Antibodies to Tg were as described previously (30).

Sequential Immunoprecipitation

Transiently transfected COS-7 cells expressing Tg-G2320R were pulse-labeled and chased as described in the text. First round immunoprecipitations were done using antibodies specific for Tg, BiP, ERp72, or PDI. After immunoprecipitation, the residual supernatants from the first round immunoprecipitation were split into three equal aliquots. A second round of immunoprecipitation was then done on these supernates using Tg-, ERp72-, or PDI-specific antibodies. Second round immunoprecipitations were carried out overnight in the presence of fresh protease inhibitors.

Endoglycosidase H Treatment

At different chase times after pulse labeling, an aliquot of transfected COS-7 cell lysates was resuspended in 0.5% SDS and 1% 2-mercaptoethanol in 20 mM Tris-HCl, pH 7.4, and boiled for 5 min. The denatured lysates were then either mock-digested or digested in the presence of 250 units of endoglycosidase H (New England Biolabs, Beverly, MA) in 50 mM sodium citrate, pH 5.5, for 1 h at 37 °C. The samples were then immunoprecipitated with an anti-Tg antibody followed by reducing SDS-PAGE and phosphorimaging.

TUNEL Staining

Paraffin-embedded wild-type and *rdw/rdw* rat thyroid paraffin sections (10 μm) were placed on coated glass slides and deparaffinized by three successive immersions in xylene for 10 min. The sections were rehydrated for 5 min each in a decreasing alcohol series (100, 90, 70% ethanol) and finally immersed in PBS for 5 min. Staining for apoptosis was performed using the TACS-XL *in situ* apoptosis detection kit (R&D Systems, Minneapolis, MN) according to the manufacturer's protocol except for the following modifications. Tissue sections were permeabilized with proteinase K for 1 h, the labeling reaction was allowed to proceed for 2 h, TACS Blue labeling was performed for 30 min, and nuclear fast red counterstaining was extended to 20 min.

RESULTS

Tg-G2320R Exhibits a Disulfide Maturation Defect

The Tg monomer forms ~60 intrachain disulfide bonds within its globular structure (17). The Tg-G2320R mutation, responsible for the dwarf phenotype of the *rdw/rdw* rat, was examined for the steady state level of Tg disulfide maturation. The full-length wild-type mouse Tg cDNA

was mutagenized to encode the G2320R mutation and this was transiently expressed in COS cells. Proteins of the transiently transfected cells were reacted with PEG-maleimide, a reagent that alkylates free thiols and adds ~5 kDa of molecular mass to each reactive cysteine thiol (31). If a sufficient number of thiols were to be alkylated, a change in the molecular mass of the 330-kDa Tg monomer would be detected by SDS-PAGE/immunoblotting as a slower migrating form. Well folded wild-type Tg migrated comparably under untreated *versus* treated conditions (Fig. 1A), and untreated Tg-G2320R migrated comparably to intracellular wild-type Tg after PEG-maleimide treatment (Fig. 1B, lanes 3 and 4), whereas PEG-maleimide treatment shifted Tg-G2320R mobility to a slower position (Fig. 1B, lane 5), indicating abnormal exposure of cysteine thiols in the mutant protein.

What are the consequences of high level expression of maturation-defective Tg-G2320R in the thyroid of *rdw/rdw* rats? By silver staining, wild-type thyroid tissue contains a more intensely staining Tg band at ~330 kDa, whereas *rdw/rdw* thyroid exhibits increased bands of 150 and 94 kDa and one or more proteins with molecular mass of ~70 kDa (Fig. 2A, marked with asterisks). Immunoblotting showed that these reflect increased levels of ER chaperones (Fig. 2B, upper three panels) along with ER oxidoreductases ERp72, PDI, and ERp57 (next three panels) as well as the lectin-like chaperone calreticulin (next panel), whereas calnexin was only modestly affected (fibronectin levels served as a loading control (last panel)). Coordinate up-regulation of ER luminal chaperones in thyrocytes expressing Tg-G2320R (32,33) is consistent with activation of the ATF6 and Ire1 stress-signaling proteins of the tripartite ER stress response (34) that have been reported to be activated in *rdw/rdw* thyroid tissue (33). To examine activation of the third ER stress-signaling protein, PERK, *rdw/rdw* rat thyroid tissue sections were immunostained with antiphospho-PERK, which reacted in excess of that found in wild-type rat thyroid tissue (Fig. 2C) indicating generalized ER stress response activation. At the same time, formation of L-thyroxine (T₄) was undetectable by anti-T₄ immunoblotting within polypeptides contained in thyroid tissue extracts of *rdw/rdw* rats (Fig. 2D). Altogether, in conjunction with earlier work, the data in Fig. 2 demonstrate a loss of thyroid hormonogenesis accompanied by full-blown activation of ER stress response pathways in the *rdw/rdw* rat thyroid gland.

Tg-G2320R (*rdw*) Mutant Thyroglobulin Is Retained Intracellularly and Degraded by ERAD

In transiently transfected COS cells, within 2 h after wild-type Tg synthesis, Tg glycans began to acquire resistance to digestion with endoglycosidase H. By contrast, the Tg-G2320R mutant did not acquire endoglycosidase H resistance even at 4 h, indicating its failure to arrive at the Golgi complex (Fig. 3A), and no *rdw* Tg was secreted (not shown). Instead, cells disposed of the mutant protein, primarily between 6 and 24 h after synthesis (Fig. 3B) when ≤10% of molecules still remained (Fig. 3C). The presence of MG132 (15 μM) greatly inhibited the intracellular degradation (Fig. 3, B and C), indicating that ERAD of Tg-G2320R involves proteasomal disposal. ERAD of another mutant, Tg-L2263P (encoded by *cog*), is known to involve an ER mannosidase/EDEM (ER degradation-enhancing α-mannoside-like protein)-sensitive pathway inhibited by kifunensine and 1-deoxymannojirimicin (20). Pretreatment of COS cells with these glycan-processing inhibitors produced similar effects on the ERAD of Tg-G2320R at 16 h of chase; kifunensine (*KF*) and 1-deoxymannojirimicin (*DMM*) clearly inhibited ERAD of Tg-G2320R, whereas castanospermine (*CAS*) was largely without effect (Fig. 3D). Brefeldin A (*BFA*), an inhibitor of ARF1-GEF (ADP-ribosylation factor 1-guanine nucleotide exchange factor) that blocks ER-to-Golgi anterograde transport, was similarly without effect on ERAD of Tg-G2320R (Fig. 3D). Based on these results, inhibitors of glycan processing and intracellular protein trafficking cannot be used to distinguish significant differences between ERAD of Tg-G2320R and Tg-L2263P mutants.

Binding of ER Chaperones and Oxidoreductases to Mutant Tg-G2320R

Following a 60-min pulse labeling, co-immunoprecipitation of wild-type Tg or Tg-G2320R mutant with ER molecular chaperones was examined at various chase times. A fraction of newly synthesized wild-type Tg was associated with BiP at 0 h chase time, and this declined precipitously even during the first hour of chase (Fig. 4A) at a time when total labeled intracellular Tg was still maintained (*upper panel*). By contrast, Tg-G2320R association with BiP did not dramatically decline over 4 h (Fig. 4A), although it did decline over 24 h (Fig. 4B) in parallel with the kinetics of ERAD (*upper panel*). In addition to BiP, an obvious increase in the early association of both ERp72 and PDI with Tg-G2320R was evident (Fig. 4A), and substantial association continued with the remaining intracellular fraction throughout the entire 24-h post-synthesis (Fig. 4B). A similar but far less dramatic increase in association of mutant Tg was also observed with ERp57 (Fig. 4A, *bottom*), but because of the relatively low Tg co-precipitation (see below), this was not pursued extensively. Similarly, small amounts of wild-type and mutant Tg-G2320R were co-immunoprecipitated with calnexin during the first 4 h after Tg synthesis (Fig. 4A); although at much later chase times, the fraction of the small amount of residual labeled intracellular mutant Tg (*upper panel*) that was bound by calnexin became proportionately larger (Fig. 4B).

As a control for these studies, when Tg was intentionally unfolded *in situ* with increasing doses of dithiothreitol prior to co-immunoprecipitation, the pattern of chaperone/oxidoreductase co-precipitation looked quite similar for wild-type Tg, Tg-G2320R, and Tg-L2263P (with all ER chaperones and oxidoreductases becoming significantly engaged as the Tg protein was increasingly denatured, Fig. 5). These data suggest that the differences shown in Fig. 4 reflect distinct chaperone preferences for Tg-G2320R rather than technical difficulties with antibody-mediated co-immunoprecipitation. Moreover, under conditions of mannosidase inhibition when mutant Tg-G2320R persists, more mutant Tg could also be found associated with BiP, ERp72, and PDI binding partners (Fig. 4C). Indeed, the *final* amount of labeled Tg-G2320R at 24 h of chase (Fig. 4B, *upper panel*) appeared to be near quantitatively coprecipitated by BiP, calnexin, ERp72, or PDI (Fig. 4B, *lower panels*).

Multiple Chaperones Interact with the Same Population of Mutant Tg Molecules

Based on the foregoing results, a sequential IP protocol (see “Experimental Procedures”) was employed to examine whether a fraction of Tg-G2320R was simultaneously associated with more than one ER oxidoreductase. A first IP with anti-Tg recovered virtually all labeled Tg at either 0 or 6 h of chase, such that essentially no additional labeled Tg could be recovered from the remaining IP-supernatant during a subsequent round of IP with any antibody (Fig. 6A, *lanes 2–4*). Similarly, the supernatant after a first IP with anti-ERp72 yielded virtually no additional Tg that could be co-precipitated in a second IP with the same antibody (Fig. 6A, *lane 7*); just as a first round anti-PDI IP yielded little additional Tg co-precipitation with a second round of anti-PDI (*lane 12*). By contrast, a second round IP with anti-Tg recovered significant additional labeled Tg that was not associated with either of these ER oxidoreductases (Fig. 6A, *lanes 6 and 10*). Most interesting, however, was that the supernatant after a first IP with anti-ERp72 did not yield additional labeled Tg that could be co-precipitated with anti-PDI (Fig. 6A, *lane 8*), and the supernatant after a first IP with anti-PDI IP did not yield appreciable labeled Tg in a second round co-precipitation with anti-ERp72 (*lane 11*). These data suggest that the fraction of labeled Tg bound to ERp72 was the same as that associated with PDI. This complex also included BiP (data not shown), indicating that multiple ER resident proteins interact with the same fraction of mutant Tg molecules.

Covalent and Noncovalent Associations between Tg-G2320R and ER Oxidoreductases, Especially ERp72

Based on the observation that Tg-G2320R contains exposed free thiols (Fig. 1) and that both PDI and ERp72 interact with Tg-G2320R (Fig. 4, Fig. 5, and Fig. 6A), we tested the extent to which mixed disulfide bonds might form between the mutant Tg and ER-resident proteins. Lysates of transfected COS cells that had been pulse-labeled and chased for up to 1 day were untreated or treated with 2% SDS to disrupt all noncovalent associations before SDS dilution followed by co-IP of labeled Tg-G2320R with anti-BiP, anti-ERp72, or anti-PDI. Essentially no Tg-G2320R could be coprecipitated with BiP after disruption of noncovalent interactions (Fig. 6B). By contrast, co-IP of a fraction of mutant Tg with ERp72 and PDI persisted even after SDS treatment (Fig. 6B). Control experiments (not shown) established that co-IP of labeled Tg was prevented by prior reduction of the cell lysate, strongly suggesting that mutant Tg was disulfide-linked to the oxidoreductases. Although representing only a modest fraction of total Tg at the zero chase time, this fraction of mutant Tg covalently associated with ERp72 (or PDI) did not decline rapidly, as occurs in rat thyrocytes during resolution of covalent adducts of wild-type Tg with ERp57 and PDI (18). Thus, by 24 h after synthesis, the mutant Tg fraction covalently associated with ERp72 closely approximated *all* residual Tg-G2320R that was refractory to ERAD (Fig. 6B). Given recent studies suggesting that ERp72 association can inhibit ERAD of mutant Tg (28), the present data seem to direct special attention to potential function(s) of ERp72 within the ER.

Demonstration of Potential ERp72 Reductase Activity in Thyrocytes

We found that when PDI and ERp72 from the ER of PC Cl3 thyrocytes (under native conditions) were incubated with PEG-maleimide (not shown), there was partitioning of PDI into discrete bands implying distinct PDI forms, each oxidized to a different extent, whereas ERp72 was more completely and uniformly alkylated. Because ERp72 Cys residues, on average, may exist in a more reduced state than do those of PDI, we tried to isolate the potential physiological consequences of ERp72 activity. PC Cl3 thyrocytes with tetracycline-inducible overexpression of ERp72 (called rtTA-7-ERp72 cells) were generated. Within 96 h of doxycycline exposure, as measured by Western blot (Fig. 7A) and immunofluorescence (Fig. 7B), these cells massively and selectively overexpressed ERp72, unlike their comparable ORP150 levels (Fig. 7A). Endogenous wild-type Tg in rtTA-7-ERp72 cells showed no appreciable change in its kinetics of acquisition of endoglycosidase H resistance (Fig. 8A) or secretion (Fig. 8B). Moreover, when cells overexpressing ERp72 were treated with tunicamycin to induce nonglycosylation of newly synthesized Tg (Fig. 8C), activation of the ER stress response (as judged by accumulation of ER chaperones) was unaffected except for ERp72, which was already substantially accumulated in doxycycline-induced cells even before tunicamycin treatment (Fig. 8D). However, when the redox environment of the ER was rendered more reducing by the incubation of live cells with up to 200 μ M dithiothreitol for 30 min, thyrocytes overexpressing ERp72 clearly exhibited increased reduction of newly synthesized Tg (Fig. 9). The data suggest that ERp72 may have the potential to act as a Tg reductase within the lumen of the thyrocyte ER.

Persistence of a Potentially Toxic Subfraction of Tg-G2320R Molecules

As ERp72 and other ER chaperones exhibited persistent binding to a subfraction of Tg-G2320R mutant molecules over 24 h (Fig. 6), it was of interest to follow the subsequent fate of these molecules. Remarkably, there was no further disposal of the ERAD-resistant Tg-G2320R molecules beyond 1 day after synthesis (Fig. 10, *upper panel*). Moreover, this subfraction continued to be near quantitatively co-precipitated with BiP, ERp72, or PDI (Fig. 10, *lower panels*), establishing that ERAD-resistant mutant Tg was bound in multi-chaperone complexes. As homozygous expression of Tg-G2320R is the only genetic difference separating the *rdw*/

rdw rat from its wild-type Wistar-Imamichi counterpart, thyroid tissue from *rdw/rdw* and wild-type rats was examined for apoptotic nicked DNA by TUNEL staining. Thyroid sections preincubated with nuclease to intentionally nick DNA yielded homogenous dark nuclear labeling, which served as a positive control (not shown), whereas no TUNEL staining was observed in wild-type rat thyroid (Fig. 11, *left*). By contrast, thyroid sections from *rdw/rdw* rats readily exhibited TUNEL-positive cells *in situ* (Fig. 11, *right*). Interestingly, TUNEL-positive staining in *rdw/rdw* thyroid was found specifically in the lumen of thyroid follicles as has been observed in other thyroid pathogenic states (36), suggesting that apoptotic/dead thyrocytes fall into this sequestered space where they cannot easily be cleared by tissue phagocytes.

DISCUSSION

Homozygous Tg-G2320R expression is responsible for congenital hypothyroidism in *rdw/rdw* rats (24,25). This mutation in the C-terminal acetylcholinesterase-like domain of Tg results in abnormal persistence of free cysteine thiols in the mutant protein (Fig. 1) and blocks thyroxine synthesis (Fig. 2D). Tg-G2320R becomes entrapped in the proximal secretory pathway where it is degraded only slowly (Fig. 3), while resulting in a strong activation of thyroidal ER stress response (Fig. 2, A–C) (33). Targeting for ERAD of Tg-G2320R includes mannose recognition/processing (Fig. 3D). The foregoing aspects appear similar to those described for the Tg mutation responsible for congenital hypothyroidism in the *cog/cog* mouse (20), Tg-L2263P (30), which is also in the C-terminal acetylcholinesterase-like homology domain (37). Nevertheless, the *cog/cog* mouse is able to exhibit thyroid hyperplasia, whereas the *rdw/rdw* rat cannot expand thyrocyte mass (26), and this is a mystery. Because different ER storage diseases include both distinct loss-of-function and gain-of-toxic-function mutants (5), it would be valuable to know whether any physical interactions between Tg-G2320R and ER-resident proteins might participate directly or indirectly in impairing expansion of thyroid cell mass via a gain-of-toxic-function.

Multiple ER chaperones and oxidoreductases interact with both wild-type Tg (21) and Tg-L2263P (38), and such interactions can participate in retention of Tg within the ER (39,40). Indeed, recent studies have shown that endogenous, wild-type Tg also forms mixed disulfides with oxidoreductases (ERp57 and PDI) in the ER (18). However, evidence suggests that these covalent adducts, especially those engaging ERp57, represent transient oxidative folding intermediates *en route* to normal Tg dimerization (18). Only when interactions of wild-type Tg with the ERp57-calreticulin-calnexin complex are blocked by pharmacological inhibition is an increase seen in mixed disulfides with PDI along with increased ERAD of a subpopulation of Tg (18). These published findings emphasize the importance of the calreticulin-ERp57 chaperone complex in productive Tg folding (17,18), with PDI perhaps being more important in the ERAD of misfolded secretory molecules (28). However, these findings (18) do not necessarily clarify why the *cog/cog* mouse develops a large goiter while the *rdw/rdw* rat fails to expand thyrocyte cell mass. We do not yet know the answer to this question but have begun to look for clues. Our current study has tried to concentrate on characterizing the interactions between ERp72 and Tg-G2320R. Our thinking is that the potential for accumulation of chaperone-bound undegraded ERAD substrate might be a critical link to cytotoxicity (12,13).

The persistence of free cysteine thiols in Tg-G2320R and the strong binding of Tg-G2320R to ERp72 do seem to highlight a special role of this ER oxidoreductase for the mutant protein (Fig. 4–Fig. 6), whereas binding to wild-type Tg is less dramatic. Under non-denaturing conditions Tg-G2320R was also co-precipitated strongly with PDI (Fig. 4–Fig. 6 and Fig. 10) and more weakly co-precipitated with ERp57 (Fig. 4A and Fig. 5). However, after exposure to denaturation with 2% SDS (which disrupts all but covalent associations), Tg-G2320R was disulfide-linked to a greater extent to ERp72 than to PDI (Fig. 6B). These findings are

particularly interesting in light of a recent report that ERAD of mutant Tg is specifically accelerated in cells overexpressing PDI and is specifically slowed in cells overexpressing ERp72 (28). More generally, PDI appears able to enhance retrotranslocation of selected ERAD substrates (such as cholera toxin A-chain), whereas ERp72 association appears to inhibit the retrotranslocation process (28). In turn, inhibition of retrotranslocation might facilitate the generation of an ERAD-resistant Tg subfraction.

Distinct ER oxidoreductases and chaperones can interact simultaneously with misfolded secretory proteins, forming large complexes (42–44). Evidence presented herein indicates that Tg-G2320R, at least in part, is also bound in multi-chaperone complexes, particularly at later chase times when co-IP using multiple different ER-resident protein antibodies each near quantitatively recovers all remaining labeled Tg (Fig. 4B, Fig. 6B, and Fig. 10). Moreover, the mere act of co-precipitating Tg-G2320R with ERp72 depletes all mutant Tg molecules engaged in interactions with PDI, and vice versa, indicating that ERp72 and PDI are associated with the same subfraction of mutant Tg (Fig. 6A). Such a result suggests a potential mechanism by which enhanced ERp72 interaction may actively interfere with PDI-facilitated Tg disposal (28).

In vitro studies have shown that PDI and ERp72 can act as either oxidases or reductases depending on the redox potential of the reaction media (46,47). The redox potential of the ER oxidoreductases *in vivo* is related to the redox environment of the ER lumen and the structure of the individual oxidoreductases. Among these, ERp72 may have an increased ability to attack disulfide bonds that have failed to be buried within the globular structure of substrates, favoring reduction of secretory proteins like Tg-G2320R (Fig. 1) via formation of disulfide cross-linked adducts (Fig. 6B). Indeed, inducible overexpression of ERp72 in PC Cl3 cells (Fig. 7), while having no significant effect on wild-type Tg export or activation of ER stress (Fig. 8), increases the potential of cells to maintain cysteine thiols of Tg in a reduced state (Fig. 9). Such activities seem to favor enhanced ERp72 interactions with misfolded mutant Tg over that of wild-type Tg (Fig. 4A), which successfully buries Cys residues within the globular structure of native Tg (21).

In this report, the interaction of ERp72 (and PDI) with Tg-G2320R at 24 h after synthesis involved nearly 100% of the remaining mutant Tg protein (Fig. 6B, *left*). At this chase time, all of the mutant Tg that was co-precipitated under nondenaturing conditions (involving both noncovalent and covalent associations with ER resident proteins) could also be co-precipitated after denaturation with 2% SDS, involving only covalent interactions (Fig. 6B, *right*). Therefore, the ERAD-resistant fraction of Tg-G2320R remaining at 24 h is engaged in disulfide linkages with ERp72 (as well as PDI). Moreover, this ERAD-resistant fraction of mutant Tg remains engaged with oxidoreductases/chaperones even 2 days post-synthesis (Fig. 10). Although this might theoretically reflect ongoing attempts to reduce Tg disulfide bonds in order to unfold the protein for retrotranslocation to the cytosol (48), it seems that the ERAD process has stalled with oxidoreductases still engaged. Thus, although increased ER chaperone and oxidoreductase expression (Fig. 2B) is thought to help limit the irreversible aggregation of misfolded secretory protein, it seems plausible that accumulation of Tg-oxidoreductase protein aggregates over time might predispose the cells to apoptotic cell death (41).

Decreased mass in *rdw/rdw* thyroid follicles might in part be attributed to the fact that, unlike wild-type rat thyroid follicles (which exhibit various sizes filled with Tg in the follicular lumen), *rdw/rdw* thyroid follicles have no accumulated Tg in the follicular lumen (26,45). Alternatively, there may be a selective disadvantage in cell growth or survival, which is consistent with independent attempts to induce high level expression of Tg-G2320R in the rtTA-7 thyrocyte cell line that have (thus far) proved unsuccessful (not shown). In human pathological specimens, studies suggest that thyrocyte apoptosis involves a loss of cellular

cohesion with neighboring thyrocytes followed by detachment of apoptotic cells into the follicular lumen (36). In this report, *rdw/rdw* rat thyroid sections showed an obvious increase in TUNEL-positive cells, especially those detected within the follicular lumen (Fig. 11). Interestingly, TUNEL-positive cells were not observed in *rdw/+* heterozygote thyroid tissue sections (data not shown), suggesting a threshold effect for levels of mutant Tg protein expression in thyrocyte cytotoxicity.

Altogether, the data in this report suggest a view that in *rdw/rdw* rats, a high level of mutant Tg-G2320R protein expression, including an undegraded fraction of molecules bound to ERp72, may predispose to thyrocyte cell death and prevent compensatory thyroid tissue expansion that would ordinarily lead to goiter. More work is needed to prove or disprove this hypothesis.

REFERENCES

1. van Anken E, Braakman I. Crit. Rev. Biochem. Mol. Biol 2005;40:191–228. [PubMed: 16126486]
2. McCracken AA, Brodsky JL. Curr. Top. Microbiol. Immunol 2005;300:17–40. [PubMed: 16573235]
3. Ellgaard L, Helenius A. Nat. Rev. Mol. Cell. Biol 2003;4:181–191. [PubMed: 12612637]
4. Rutishauser J, Spiess M. Swiss Med. Wkly 2002;132:211–222. [PubMed: 12087487]
5. Kim PS, Arvan P. Endocr. Rev 1998;19:173–202. [PubMed: 9570036]
6. Wu J, Kaufman RJ. Cell Death Differ 2006;13:374–384. [PubMed: 16397578]
7. Sekijima Y, Wiseman RL, Matteson J, Hammarstrom P, Miller SR, Sawkar AR, Balch WE, Kelly JW. Cell 2005;121:73–85. [PubMed: 15820680]
8. Chen Y, Bellamy WP, Seabra MC, Field MC, Ali BR. Hum. Mol. Genet 2005;14:2559–2569. [PubMed: 16049033]
9. Meusser B, Hirsch C, Jarosch E, Sommer T. Nat. Cell Biol 2005;7:766–772. [PubMed: 16056268]
10. Nishikawa S, Brodsky JL, Nakatsukasa K. J. Biochem 2005;137:551–555. [PubMed: 15944407]
11. Kostova Z, Wolf DH. EMBO J 2003;22:2309–2317. [PubMed: 12743025]
12. Russell TA, Ito M, Ito M, Yu RN, Martinson FA, Weiss J, Jameson JL. J. Clin. Investig 2003;112:1697–1706. [PubMed: 14660745]
13. Perlmutter DH. Methods Mol. Biol 2003;232:39–56. [PubMed: 12840538]
14. Kim PS, Arvan P. J. Biol. Chem 1991;266:12412–12418. [PubMed: 2061316]
15. Kim P, Bole D, Arvan P. J. Cell Biol 1992;118:541–549. [PubMed: 1353499]
16. Kim PS, Arvan P. J. Cell Biol 1995;128:29–38. [PubMed: 7822419]
17. Di Jeso B, Ulianich L, Pacifico F, Leonardi A, Vito P, Consiglio E, Formisano S, Arvan P. Biochem. J 2003;370:449–458. [PubMed: 12401114]
18. Di Jeso B, Park Y-n, Ulianich L, Treglia AS, Urbanas ML, High S, Arvan P. Mol. Cell. Biol 2005;25:9793–9805. [PubMed: 16260597]
19. Medeiros-Neto G, Kim PS, Yoo SE, Vono J, Targovnik H, Camargo R, Hossain SA, Arvan P. J. Clin. Investig 1996;98:2838–2844. [PubMed: 8981932]
20. Tokunaga F, Brostrom C, Koide T, Arvan P. J. Biol. Chem 2000;275:40757–40764. [PubMed: 10984471]
21. Di Jeso, B.; Arvan, P. The Thyroid. 9th Ed. Braverman, LE.; Utiger, R., editors. Philadelphia: Lippincott Williams & Wilkins; 2004.
22. Ahlbom BE, Yaqoob M, Gustavsson P, Abbas HG, Anneren G, Larsson A, Wadelius C. Hum. Genet 2002;110:145–147. [PubMed: 11935320]
23. Koto M, Sato T, Okamoto M, Adachi J. Exp. Anim 1988;37:21–30.
24. Kim PS, Ding M, Menon S, Jung CG, Cheng JM, Miyamoto T, Li B, Furudate S, Agui T. Mol. Endocrinol 2000;14:1944–1953. [PubMed: 11117525]
25. Hishinuma A, Furudate S, Oh-Ishi M, Nagakubo N, Namatame T, Ieiri T. Endocrinology 2000;141:4050–4055. [PubMed: 11089535]
26. Umezu M, Kagabu S, Jiang J, Sato E. Lab. Anim. Sci 1998;48:496–501. [PubMed: 10090064]

27. Carelli S, Ceriotti A, Cabibbo A, Fassina G, Ruvo M, Sitia R. *Science* 1997;277:1681–1684. [PubMed: 9287224]
28. Forster ML, Sivick K, Park YN, Arvan P, Lencer WI, Tsai B. *J. Cell Biol* 2006;173:853–859. [PubMed: 16785320]
29. Caldwell SR, Hill KJ, Cooper AA. *J. Biol. Chem* 2001;276:23296–23303. [PubMed: 11316816]
30. Kim PS, Hossain SA, Park Y-N, Lee I, Yoo S-E, Arvan P. *Proc. Natl. Acad. Sci. (U. S. A.)* 1998;95:9909–9913. [PubMed: 9707574]
31. Tsai B, Rodighiero C, Lencer WI, Rapoport TA. *Cell* 2001;104:937–948. [PubMed: 11290330]
32. Oh-Ishi M, Omori A, Kwon JY, Agui T, Maeda T, Furudate SI. *Endocrinology* 1998;139:1288–1299. [PubMed: 9492064]
33. Baryshev M, Sargsyan E, Wallin G, Lejniaks A, Furudate S, Hishinuma A, Mkrtchian S. *J. Mol. Endocrinol* 2004;32:903–920. [PubMed: 15171721]
34. Schroder M, Kaufman RJ. *Annu. Rev. Biochem* 2005;74:739–789. [PubMed: 15952902]
35. Knauf JA, Kuroda H, Basu S, Fagin JA. *Oncogene* 2003;22:4406–4412. [PubMed: 12853977]
36. Labat-Moleur F, Chabre O, Guillermet C, Chaffanjon P, Blumet-Rondeu F, Bauchet A, Franc S, Brambilla E, Bachelot I, Dumont JE, Negoescu A. *Thyroid* 1999;9:483–492. [PubMed: 10365680]
37. Park YN, Arvan P. *J. Biol. Chem* 2004;279:17085–17089. [PubMed: 14764582]
38. Kim PS, Kwon O-Y, Arvan P. *J. Cell Biol* 1996;133:517–527. [PubMed: 8636228]
39. Muresan Z, Arvan P. *J. Biol. Chem* 1997;272:26095–26102. [PubMed: 9334173]
40. Muresan Z, Arvan P. *Mol. Endocrinol* 1998;12:458–467. [PubMed: 9514162]
41. Bucciantini M, Giannoni E, Chiti F, Baroni F, Formigli L, Zurdo J, Taddei N, Ramponi G, Dobson CM, Stefani M. *Nature* 2002;416:507–511. [PubMed: 11932737]
42. Molinari M, Galli C, Piccaluga V, Pieren M, Paganetti P. *J. Cell Biol* 2002;158:247–257. [PubMed: 12119363]
43. Kuznetsov G, Chen LB, Nigam SK. *J. Biol. Chem* 1997;272:3057–3063. [PubMed: 9006956]
44. Anelli T, Alessio M, Bachi A, Bergamelli L, Bertoli G, Camerini S, Mezghrani A, Ruffato E, Simmen T, Sitia R. *EMBO J* 2003;22:5015–5022. [PubMed: 14517240]
45. Sakai Y, Yamashina S, Furudate SI. *Anat. Rec* 2000;259:60–66. [PubMed: 10760744]
46. Rupp K, Birnbach U, Lundstrom J, Van PN, Soling HD. *J. Biol. Chem* 1994;269:2501–2507. [PubMed: 8300576]
47. Lundstrom-Ljung J, Birnbach U, Rupp K, Soling HD, Holmgren A. *FEBS Lett* 1995;357:305–308. [PubMed: 7835433]
48. Fagioli C, Mezghrani A, Sitia R. *J. Biol. Chem* 2001;276:40962–40967. [PubMed: 11533039]

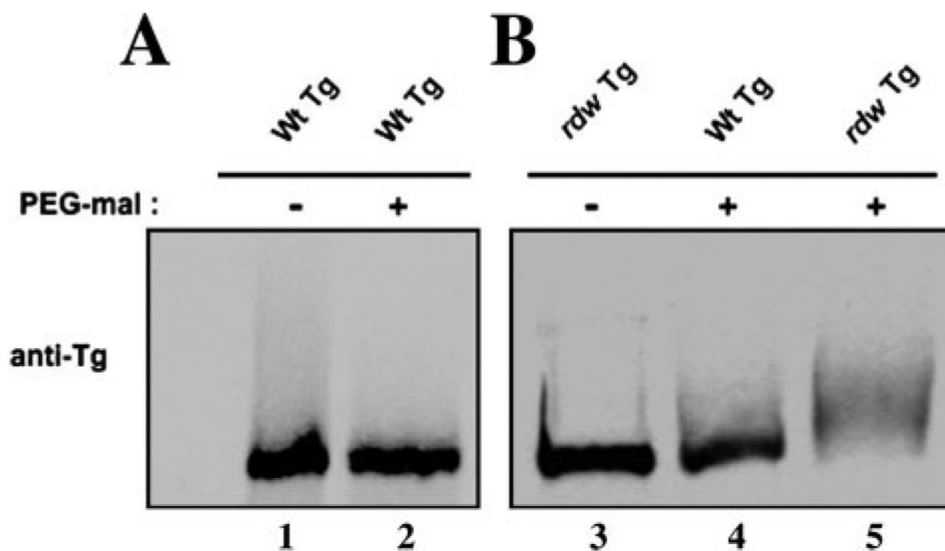


FIGURE 1. Disulfide maturation defect for Tg-G2320R

COS-7 cells were transfected with either wild-type (*Wt*) or *rdw* Tg cDNA, and protein levels of the respective proteins by immunoblotting were comparable as reported previously (24). *A*, well folded wild-type Tg secreted from COS cells did not exhibit any mobility shift upon treatment with 10 mM mPEG 5000-maleimide for 75 min. The samples were then analyzed by reducing SDS-4% PAGE followed by immunoblotting with anti-Tg. *B*, intracellular proteins from the transiently transfected cells were reacted with 10 mM mPEG 5000-maleimide for 75 min. The samples were analyzed as described in *A*. Under these conditions, as a consequence of the presence of the G2320R mutation, PEG-maleimide caused mutant Tg to appear as a slower migrating form, whereas the wild-type Tg band was shifted much less.

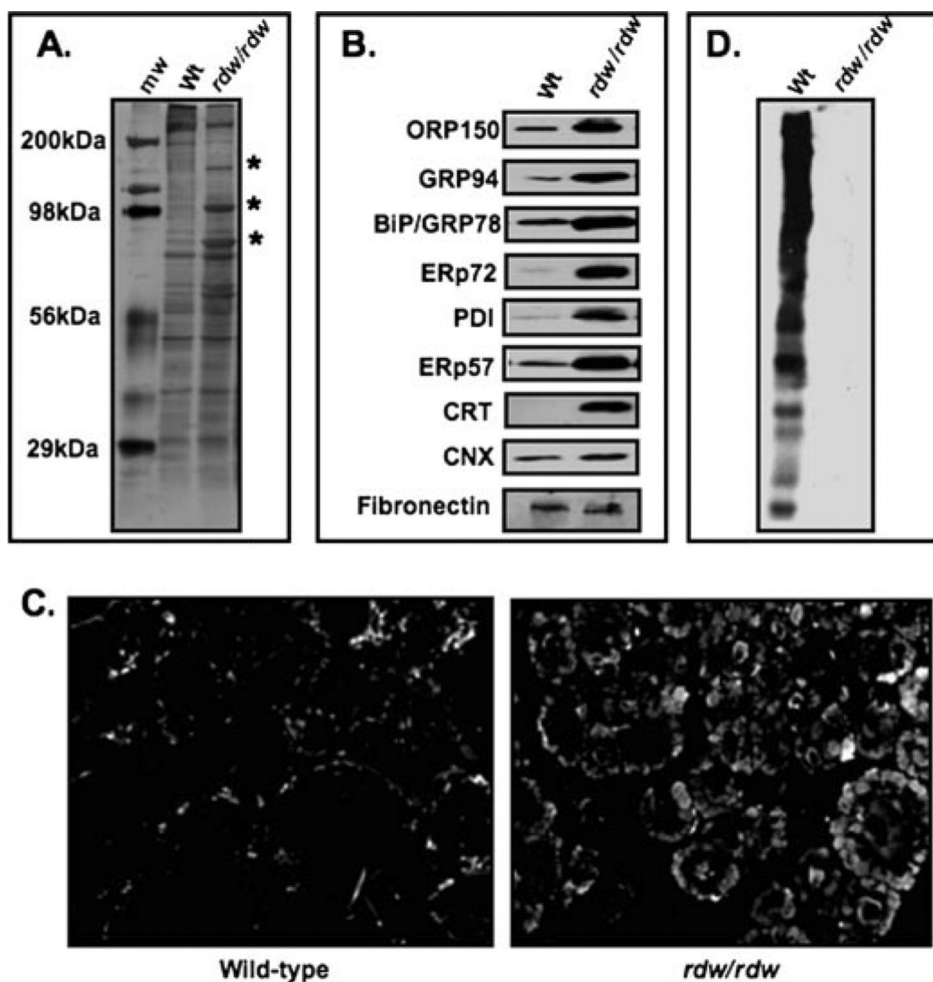


FIGURE 2. Protein and hormone content of *rdw/rdw* rat thyroid tissue

A, 100 μ g of protein from thyroid tissue homogenates of wild-type (*Wt*) and *rdw/rdw* rats was analyzed by SDS-7% PAGE; the proteins were silver-stained. An ~330-kDa band near the top of the gel is consistent with the presence of Tg. Thyroid tissue from *rdw/rdw* rats displays abnormally increased bands (*asterisks*); the corresponding molecular weights (*mw*) suggest up-regulation of known ER molecular chaperones. The positions of molecular mass standards are shown at *left*. B, Western blotting for ER molecular chaperones in thyroid tissues from wild-type and *rdw/rdw* rats. *CNX*, calnexin; *CRT*, calreticulin. Fibronectin was measured as a loading control. C, wild-type and *rdw/rdw* rat thyroid sections stained with antiphospho-PERK; thyrocytes from the mutant showed enhanced staining. D, 100 μ g of thyroid tissue protein from wild-type and *rdw* rats was probed with an antibody specific for T₄. Many bands representing intact and proteolytically cleaved Tg from normal thyroid tissue contained preformed thyroid hormone, whereas *rdw/rdw* thyroid appeared devoid of thyroxine. The positions of molecular mass standards are the same as those shown in A.

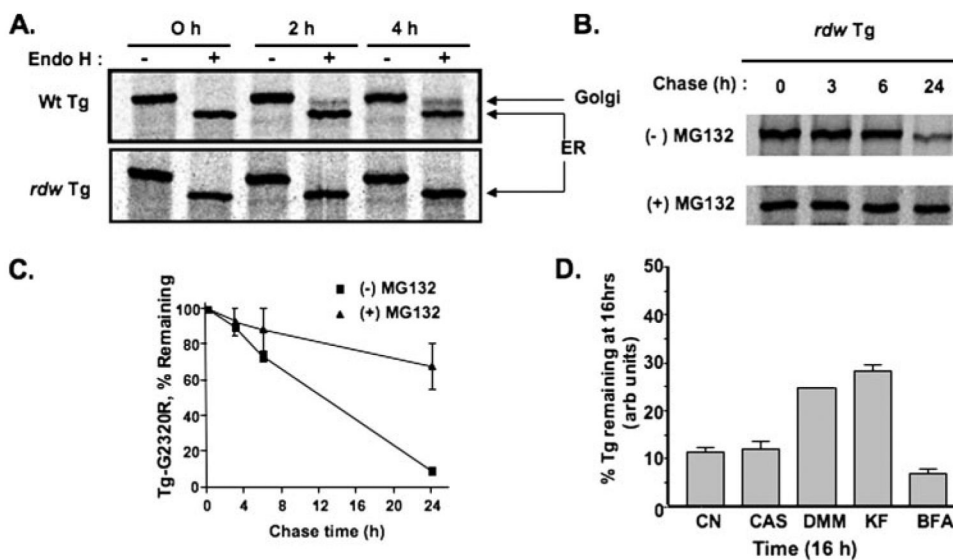


FIGURE 3. Tg-G2320R is intracellularly retained and degraded by proteasomes

COS-7 cells transiently transfected to express wild-type (*Wt*) or *rdw* Tg were pulse-labeled with ^{35}S -labeled amino acids and chased for various times. *A*, acquisition of endoglycosidase H (*Endo H*) resistance. No Tg-G2320R mutant reached the medial Golgi complex even at 4 h after synthesis. Note that wild-type (*Wt*) Tg does not accumulate intracellularly as an endoglycosidase H-resistant form because of secretion to the medium. *B*, degradation of Tg-G2320R in the absence and presence of 15 μM MG-132, a proteasomal inhibitor. *C*, quantitation of the experiment shown in *B*. *D*, quantitation of the fraction of newly synthesized mutant Tg-G2320R remaining at 16 h under control conditions (*CN*) or in the presence of 1 mM castanospermine (*CAS*), 1 mM deoxymannojirimycin (*DMM*), 100 μM kifunensine (*KF*), or 10 $\mu\text{g/ml}$ brefeldin A (*BFA*). Each drug was also included in a 30-min pretreatment period prior to metabolic labeling.

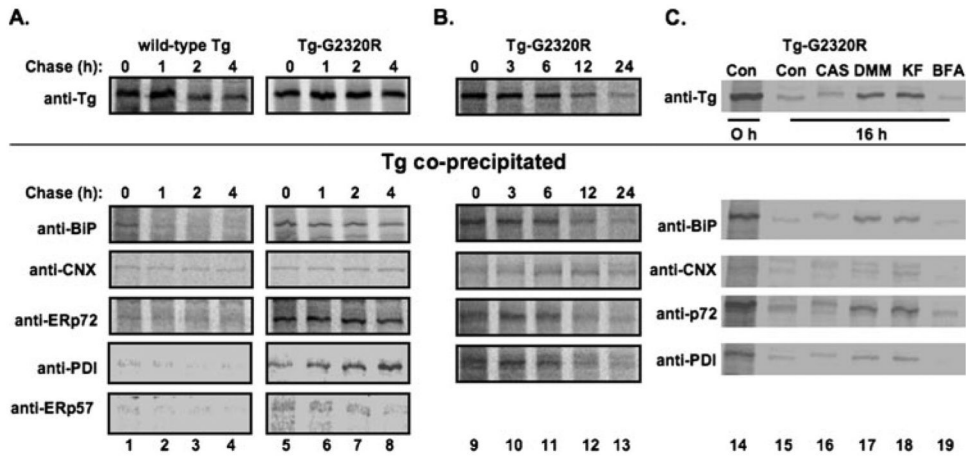


FIGURE 4. Interactions of ER chaperones and oxidoreductases with Tg-G2320R in transiently transfected COS-7 cells

A, direct immunoprecipitation and co-immunoprecipitation of Tg carried out using either Tg-, BiP-, calnexin (CNX)-, ERp72-, PDI-, or ERp57-specific antibodies. Cells transfected to express either wild-type Tg or Tg-G2320R were pulse-labeled with ^{35}S -labeled amino acids for 60 min and chased for the times indicated before lysis in a 1% Triton X-100-containing buffer (see “Experimental Procedures”) and immunoprecipitation with the indicated antibodies. Co-precipitation of wild-type Tg with ER chaperones and oxidoreductases was at low levels or at levels that declined with time, whereas co-precipitation of Tg-G2320R was at higher levels or at levels that tended to persist over a 4-h chase period. Because anti-calnexin co-immunoprecipitated many other bands in COS-7 cells, the calnexin immunoprecipitates were denatured and reimmunoprecipitated with anti-Tg prior to SDS-PAGE. B, Tg-G2320R interactions with BiP, ERp72, PDI, and calnexin (*lower panels*) exhibit extended kinetics that match the life span of the mutant Tg protein in cells (*upper panel*). C, Tg-G2320R immunoprecipitation and co-precipitation with ER chaperones/oxidoreductases under control conditions (*Con*) or in cells treated with 1 mM castanospermine (*CAS*), 1 mM deoxymannojirimycin (*DMM*), 100 μM kifunensine (*KF*), or 10 $\mu\text{g/ml}$ brefeldin A (*BFA*). Each drug was also included in a 30-min pretreatment period prior to metabolic labeling.

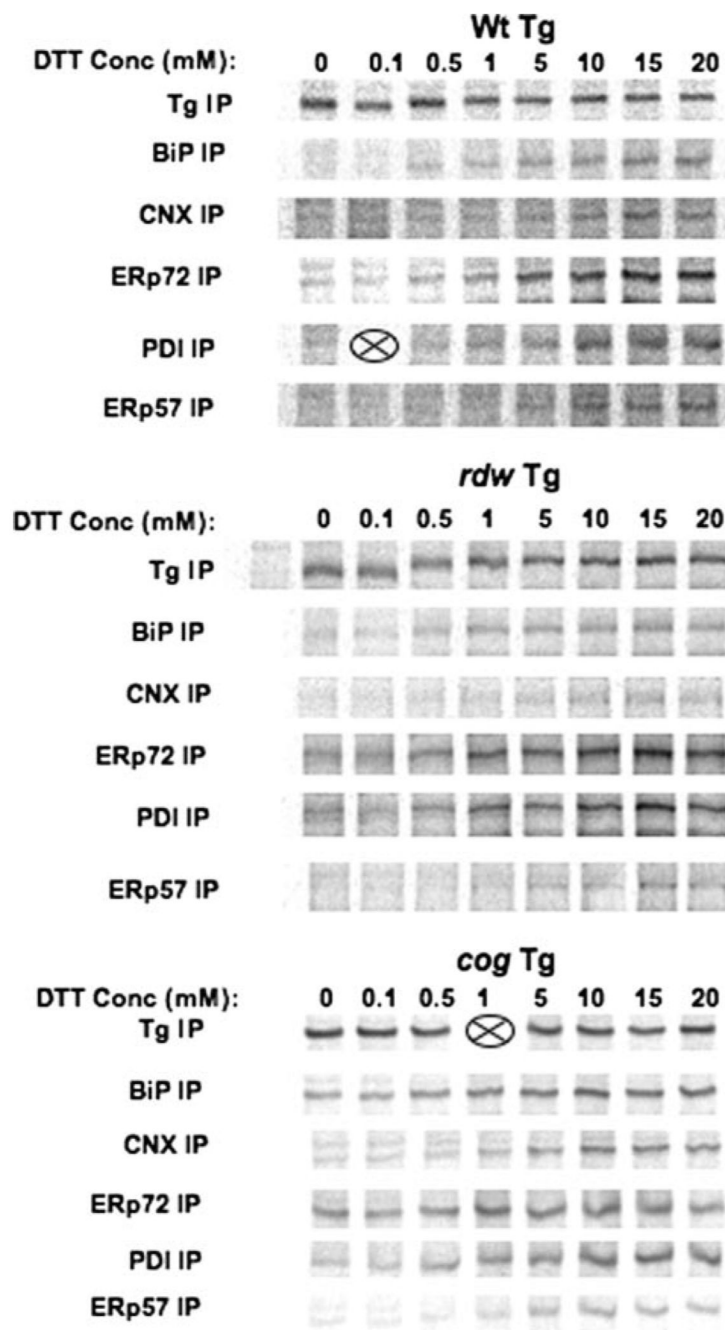


FIGURE 5. Co-immunoprecipitation of wild-type (*Wt*) or mutant Tg with ER chaperones and oxidoreductases after pharmacological unfolding of Tg with dithiothreitol

COS-7 cells transiently transfected to express the indicated Tg proteins were labeled for 30 min with ^{35}S -labeled amino acids, washed, and then chased for 30 min in media containing varying concentrations of dithiothreitol (*DTT*) as shown. The live cells were then washed in PBS and treated with iodoacetamide before lysis and immunoprecipitation with the indicated antibodies. Two samples were lost during processing (indicated by *X*). *CNX*, calnexin.

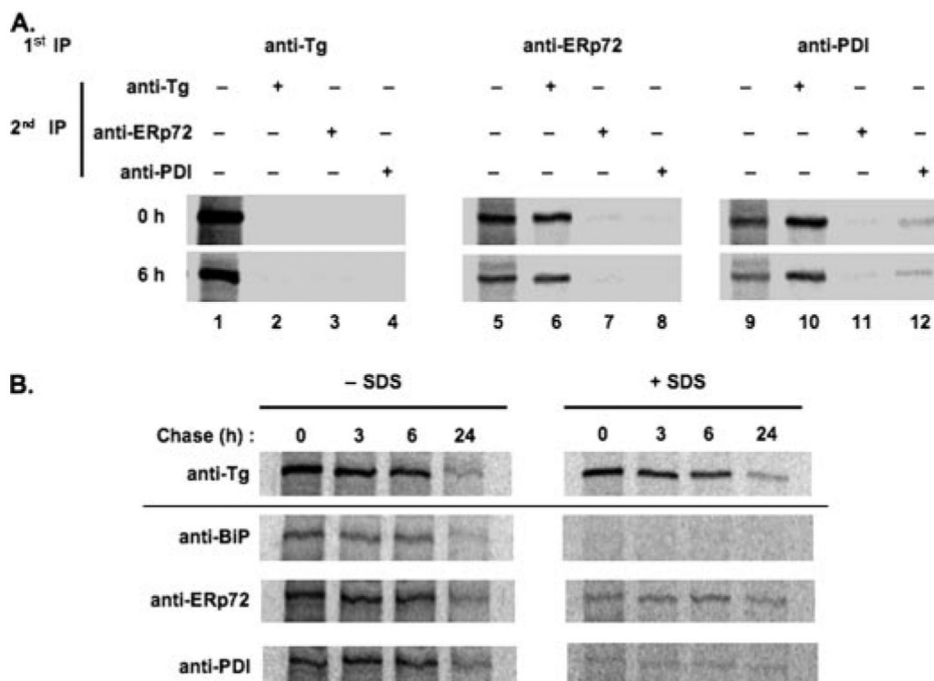


FIGURE 6. ER oxidoreductases interact simultaneously and covalently with Tg-G2320R

A, transiently transfected COS-7 cells expressing Tg-G2320R were pulse-labeled and chased for 0 and 6 h. Cells were lysed and first immunoprecipitated with an antibody against Tg, ERp72, or PDI as indicated; the recovered Tg was analyzed in lanes 1, 5, and 9, respectively. The supernates of these IPs were then used as the starting material for a fresh second round of immunoprecipitation with antibodies against Tg, ERp72, or PDI. First and second round immunoprecipitates were analyzed by reducing SDS-4% PAGE and phosphorimaging. Only the labeled Tg band recovered is shown. B, transiently transfected COS-7 cells were pulse-labeled and chased for the times shown before cell lysis on ice for 1 h in the presence of apyrase (see “Experimental Procedures”). After a brief centrifugation to remove cell debris, the lysate was split into two equal portions; one was left untreated (*left panels*), and SDS was added to the other to a final concentration of 2% (*right panels*). After a 30-min incubation, all samples were diluted 10-fold in buffer lacking SDS (but containing 1% Triton X-100) prior to immunoprecipitation with the antibodies shown.

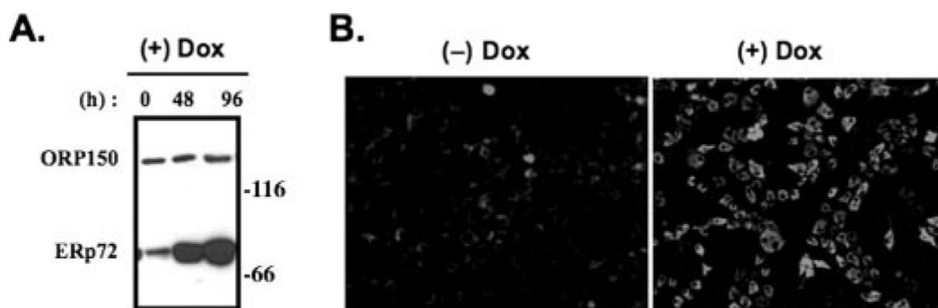


FIGURE 7. Tetracycline-inducible overexpression of ERp72 in a thyrocyte cell line
A, after treatment with doxycycline (*Dox*) for 48 or 96 h as indicated, rtTA-7-ERp72 cells were lysed and immunoblotted with antibodies for ORP150 and ERp72. The positions of molecular mass markers are shown at *right*. B, 96 h after doxycycline exposure, the cells were processed for immunofluorescence with a primary antibody against ERp72. Comparable numbers of cells are shown in each field.

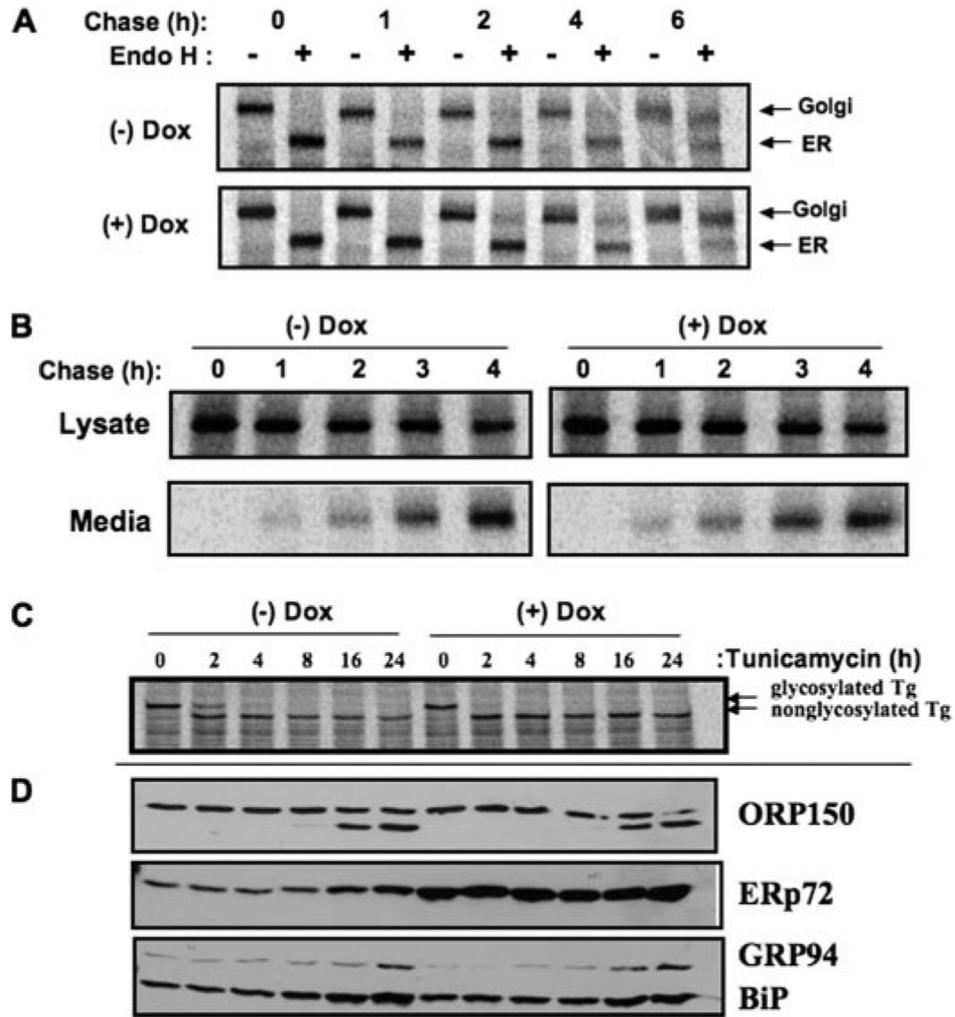


FIGURE 8. Absence of global ER phenotypes in thyrocytes overexpressing ERp72

A, rtTA-7-ERp72 cells, either uninduced or induced to overexpress ERp72 by 96 h of doxycycline (*Dox*) treatment, were pulse-labeled with ^{35}S -labeled amino acids for 30 min and chased for the indicated times. At each chase time, the total labeled Tg recovered by immunoprecipitation was either undigested or digested with endoglycosidase H (*Endo H*). The samples were analyzed by SDS-PAGE and phosphorimaging. *B*, using a protocol similar to that for described for *A*, labeled Tg recovered from cells (*Lysate*) or media were analyzed as a function of chase time. *C* and *D*, rtTA-7-ERp72 cells, either uninduced or induced to overexpress ERp72 by 96 h of doxycycline treatment, were treated with tunicamycin continuously for 24 h. At different times of treatment cells were pulse-labeled with ^{35}S -labeled amino acids for 30 min without chase, and newly synthesized Tg was immunoprecipitated and analyzed by SDS-PAGE (*C*); or cells were lysed and analyzed by Western blotting for ER chaperones ORP150, ERp72, GRP94, or BiP as shown (*D*).

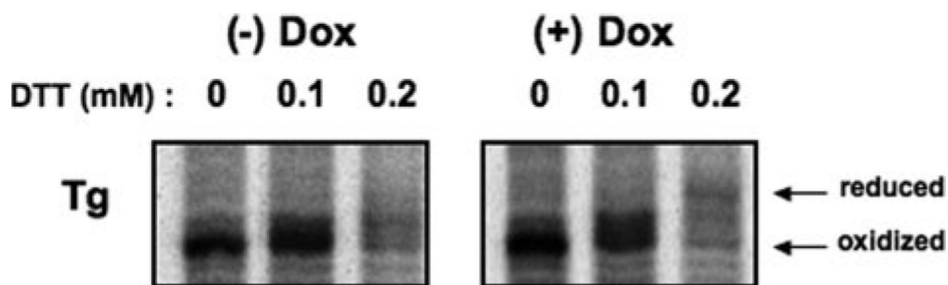


FIGURE 9. Ability of ERp72-overexpressing thyrocytes to reduce Tg disulfide Bonds
rtTA-7-ERp72 cells, either uninduced or induced to overexpress ERp72 by 96 h of doxycycline treatment (*Dox*), were pulse-labeled with ^{35}S -labeled amino acids for 30 min in the presence of dithiothreitol (*DTT*) at the concentrations shown. At the end of the labeling period, *in situ* reduction was terminated by the addition of *N*-ethylmaleimide, and the cells were lysed, immunoprecipitated for Tg, and analyzed by SDS-PAGE and phosphorimaging.

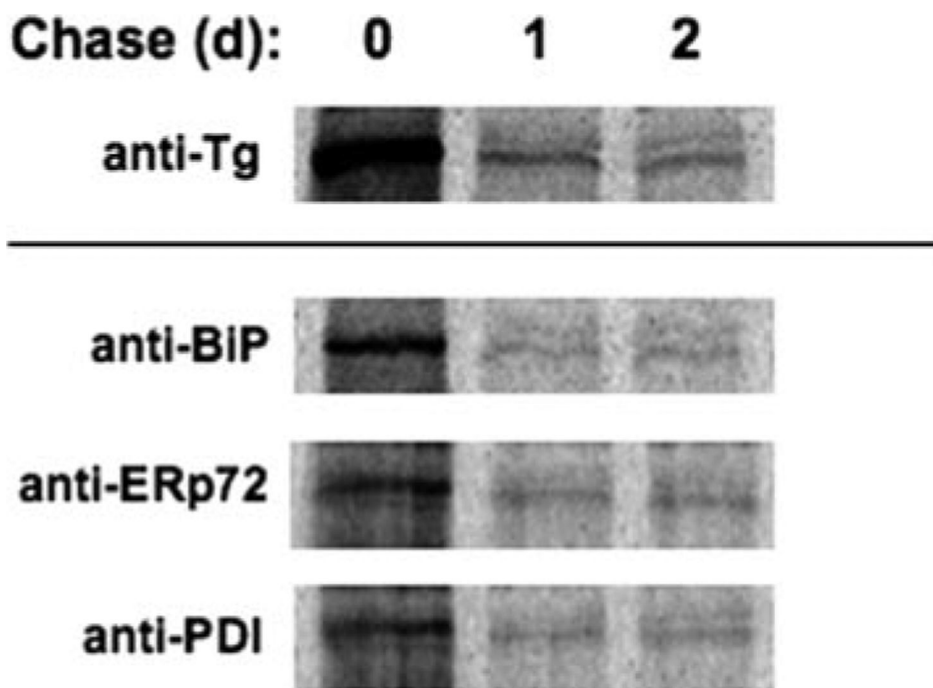


FIGURE 10. The fraction of mutant Tg remaining at 24 h of chase is refractory to ERAD
Pulse-labeled COS-7 cells that had been transfected to express Tg-G2320R were chased for the indicated times (*d*, days) before direct immunoprecipitation with anti-Tg (*upper panel*) or co-precipitation with ER-resident proteins (*lower panels*).

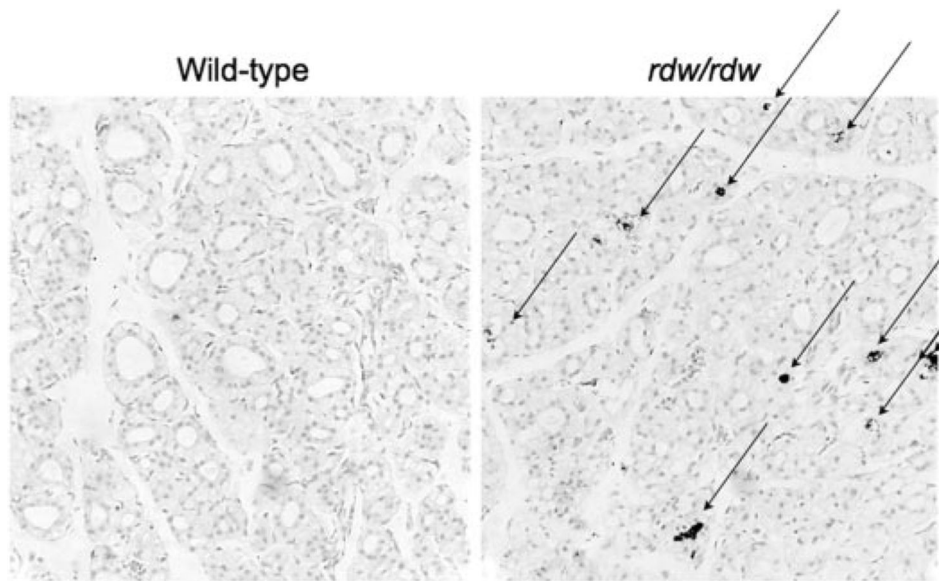


FIGURE 11. Detection of apoptosis in *rdw* thyroid sections

TUNEL staining of thyroid tissue sections was performed with the TACS-XL *in situ* apoptosis detection kit. Nuclei were counterstained with fast red. Although no positive staining was detected in wild-type thyroid tissue (*left*), positive staining (*arrows*) was detected in *rdw/rdw* thyroid tissue, with most staining found in the follicular lumen.